Dynamics of a Polymer/Diluent System As Studied by Dielectric Spectroscopy and Neutron Scattering

G. Floudas*,† and J. S. Higgins

Department of Chemical Engineering, Imperial College, London SW7 2BY, England

F. Kremer and E. W. Fischer

Max-Planck-Institut für Polymerforschung, D-6500 Mainz, Germany

Received March 9, 1992; Revised Manuscript Received May 22, 1992

ABSTRACT: Dielectric spectroscopy and incoherent neutron scattering are employed to study the dynamics of concentrated solutions of solution-chlorinated polyethylene with bis(2-ethylhexyl) phthalate. The dielectric measurements were made at temperatures (T) between 200 and 435 K and in the frequency range from 10^{-1} to 10^9 Hz. The incoherent neutron scattering measurements covered the T range between 4 and 400 K and the Q range from 0.33 to 1.84 Å^{-1}. From dielectric spectroscopy (DS) we obtain the T dependence (i) of the dynamics and (ii) of the distribution of relaxation times over a broad frequency/temperature range. Our results for the dynamics are discussed in terms of the Vogel–Fulcher–Tammann (VFT) approach with a single primary (α) relaxation affecting the DS data. Our results for the distribution of relaxation times, obtained either in the frequency domain or in the time domain, display a systematic T dependence with significantly broader distributions for the mixtures, at low T, as compared to the bulk polymer and the neat solvent. This is discussed in terms of theoretical models which predict a narrowing of the distribution with increasing T. From the neutron scattering experiment, made on the same samples but at a higher frequency range, we obtained evidence for enhanced proton mobility with T, setting in at about the characteristic temperature (T_0) of the VFT approach.

Introduction

The primary (α) glass–rubber relaxation in amorphous polymers is associated with cooperative segmental motions. To describe the behavior of such motions, different theoretical models[1–4] and a variety of experimental techniques have been used.[5] The central point in the theoretical models is that of a domain, made up from cooperatively moving segments, whose number increases with decreasing temperature (T). The number of cooperative segments diverges at some temperature T_0, close to but below the observed glass transition temperature T_g. Usually a non-Arrhenius empirical equation (Vogel–Fulcher–Tammann) is used to describe the T dependence of the relaxation time τ above T_g, and T_0 is obtained by extrapolation. Furthermore, a variety of glass-forming systems (polymeric and nonpolymeric) and characterized by a broad distribution of relaxation times rather than a single relaxation time. Theoretical models predict that the distribution of relaxation times changes in a systematic way with T.[6–9] For example, in the fluctuation approach,[4,6] the width of the distribution diverges as we approach T_0. However, in the mode coupling approach,[10] time–temperature superposition is essential at least in a temperature range above the critical temperature, T_c.

To properly characterize relaxations with a broad distribution of relaxation times, the T dependence of (i) τ and of (ii) the distribution is needed over a broad frequency/temperature range. However, only a few experimental techniques have a sufficiently broad dynamic range, so it is necessary to combine data from different experiments which may or may not probe the same properties. Although successful comparisons have been made before, mainly with the use of light scattering,[11] dielectric relaxation,[12,13] and ultrasonic relaxation,[14] there have been indications for the decoupling of different degrees of freedom as probed by different experiments.[15]

The purpose of the present work is to study the dynamics of a polymer/diluent system over a broad frequency/temperature range. For this purpose we employ broad-band (10^{-1}–10^9 Hz) dielectric relaxation spectroscopy (DS) on the polymer/diluent system solution-chlorinated polyethylene/bis(2-ethylhexyl) phthalate (SCPE/DOP) and for polymer concentrations higher than 59%. In this way we obtain (i) the temperature dependence of the dynamics and (ii) the distribution of relaxation times over a broad frequency/temperature range. We discuss our results for the dynamics in terms of the Vogel–Fulcher–Tammann (VFT)–free volume approach with a single primary (α) relaxation process affecting the DS data. Our results for the T dependence of the distribution are discussed in terms of recent theoretical models.

In dynamic experiments the temperature T_0 is not easily experimentally accessible. However, by monitoring the elastically scattered intensity in the incoherent neutron scattering experiment, we can study the mobility of the system in the vicinity of T_0. In the present system we find an increasing proton mobility at T below T_g and surprisingly in the vicinity of T_0. The correlation between proton mobility, as obtained from a static property (intensity) and T_0, as obtained from dynamic experiments on the same samples—which is reported here for the first time—constitutes the main result of the present study.

Experimental Section

Materials. Solution-chlorinated polyethylene ($M_W \sim 2 \times 10^5$) was prepared from linear polyethylene (PE) using the procedure described elsewhere.[16] The chlorine content of the SCPE was found by elemental analysis to be 56.6% w/w. In contrast to suspension-chlorinated PE, the SCPE sample is amorphous due to the random distribution of chlorine atoms along the chain. This was verified by the X-ray scattering pattern, which consists of a halo characteristic of amorphous polymers. Three concentrated solutions with bis(2-ethylhexyl) phthalate (DOP); (Aldrich) were prepared gravimetrically (by direct addition to solvent of polymer) with polymer contents 88, 74, and 59%. The glass transition temperatures T_g, determined by differential scanning calorimetry (DSC) at a heating rate of 10

* Author to whom correspondence is addressed.
† Present address: Max-Planck-Institut für Polymerforschung, Postfach 3148, D-6500 Mainz, Germany.

0024-9297/92/2225-4955$03.00/0

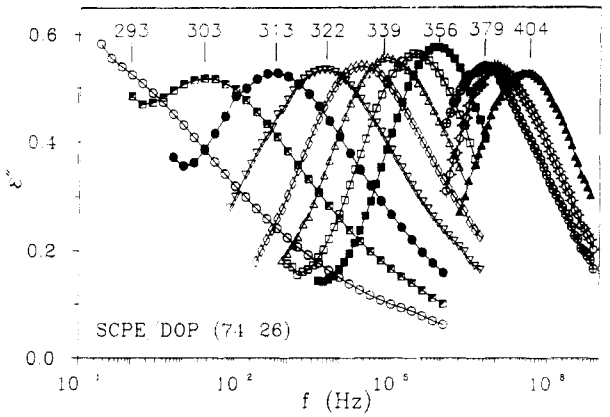

Figure 1. Dielectric loss ϵ'' versus frequency for the plasticized SCPE with 26% DOP at different temperatures as indicated.

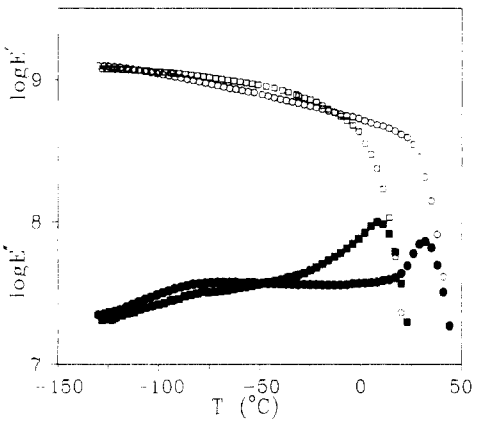

Figure 2. Storage E' (open symbols) and loss E'' (solid symbols) moduli at 1 Hz as a function of temperature for bulk (○, ●) and plasticized (□, ■) SCPE with 26% DOP.

K min^{-1}, were 317, 295, 279, and 245 K respectively for the bulk and plasticized SCPE with 12, 26, and 41% DOP. There was no evidence of a second glass transition in the DSC measurements in the temperature range from 120 to 420 K. However, the breadth of the transition increases with increasing DOP content from 16 K for the bulk SCPE to ~24 K for the SCPE/DOP (59/41) sample. The shift of the glass transition to lower temperatures and the broadening of the transition are typical of polymer/additive systems.

Dielectric Spectroscopy. The dielectric measurements were made in the frequency range from 10^{-1} to 10^{9} Hz. To cover this frequency range, three measurement systems were employed: (i) a frequency response analyzer (Solartron Schlumberger 1254), (ii) an automatic low-frequency bridge (Hewlett-Packard 4192A), and (iii) an impedance analyzer (Hewlett-Packard 4191A) based on the principle of a coaxial line reflectometer. The samples were kept within two gold-plated stainless-steel plates of 20-mm diameter, with a separation of ~50 μm being maintained by fused-silica spacers. The sample temperature was adjusted by a jet of temperature-controlled nitrogen gas in the temperature range 200–435 K, with a stability better than ±0.1 K. Details of the experimental setup can be found in ref 17. Typical dielectric relaxation loss curves (ϵ'') for the system SCPE/DOP (74/26) obtained with the three systems described above are shown in Figure 1.

Complementary dynamic mechanical measurements were made with (i) a standard dynamic mechanical thermal analyzer (DMTA, Polymer Laboratories) and (ii) a Rheometrics RMS 800 spectrometer. The DMTA spectrometer was used in the tensile mode, giving the storage modulus E' and loss modulus E'' (E = Young's modulus) for the bulk SCPE and the SCPE/DOP (74/26) sample in the T range from 140 to 360 K, at 1 Hz (Figure 2). The Rheometrics spectrometer was used in the shear mode, giving the storage modulus G' and loss modulus G'' for the bulk SCPE in the T range from 113 to 373 K and for 10 frequencies between 0.1 and 100 rad/s.

Neutron Scattering. The neutron scattering measurements were carried out on the IRIS back-scattering spectrometer at the

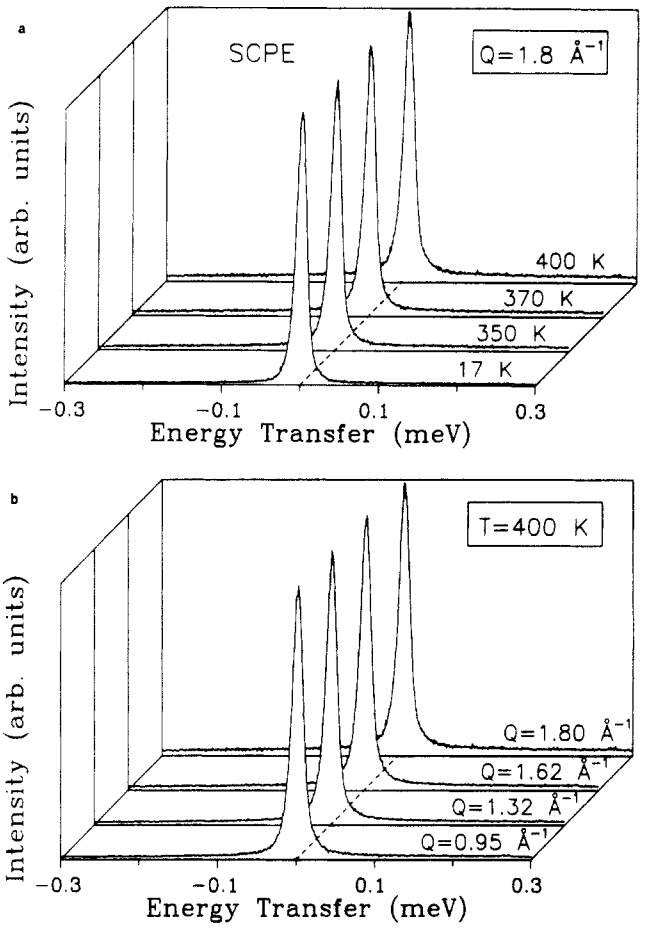

Figure 3. Incoherent neutron scattering spectra of SCPE (a) as a function of T and (b) as a function of Q. The lowest measured temperature (T = 17 K) is the spectrometer resolution function.

ISIS pulsed neutron source at the Rutherford Appleton Laboratory (RAL). Two samples were used in the neutron scattering experiment: the bulk and plasticized SCPE with a polymer concentration of 74%. The samples were contained in a flat Al container, and the sample thickness was set to 0.2 mm—in order to suppress multiple scattering—resulting in a transmission of 89%. The Al container was then mounted in a variable-temperature liquid-helium cryostat at 45° to the incident beam. The energy resolution of the spectrometer was 11 μeV (fwhh) and the energy range from −0.4 to +0.4 meV. Measurements were made in the temperature range 4–400 K and over the Q range 0.33–1.84 Å^{-1}. Typical spectra for the bulk polymer as a function of T and Q are shown in Figure 3 and for the SCPE/DOP (74/26) sample in Figure 4.

Data Analysis

The dielectric relaxation data for the frequency-dependent complex dielectric permittivity ($\epsilon^*(\omega) = \epsilon'(\omega) - i\epsilon''(\omega)$) include contributions from both dc conduction and relaxation. The rise of $\epsilon''(f)$ in Figures 1 and 5 at low frequencies is caused by the electrical conductivity of the material which can be fitted according to $\epsilon'' \sim (\sigma_0/\epsilon_0)\omega^{s-1}$, where σ_0 and s ($0 \le s \le 1$) are fitting parameters and ϵ_0 denotes the permittivity of free space. The relaxation part of the dielectric loss has been fitted (Figure 5) to the empirical equation of Havriliak–Negami (HN)[18]

$$\epsilon^*(\omega) = \epsilon_\infty + \frac{\epsilon_0 - \epsilon_\infty}{[1 + (i\omega\tau_{HN})^\alpha]^\gamma} \quad (0 < \alpha, \gamma \le 1) \quad (1)$$

where ϵ_0 and ϵ_∞ are respectively the low- and high-frequency values of the real part of the dielectric permittivity and τ_{HN} is the characteristic relaxation time. The parameters α and γ describe respectively the symmetrical and asymmetrical broadening of the distribution of relaxation

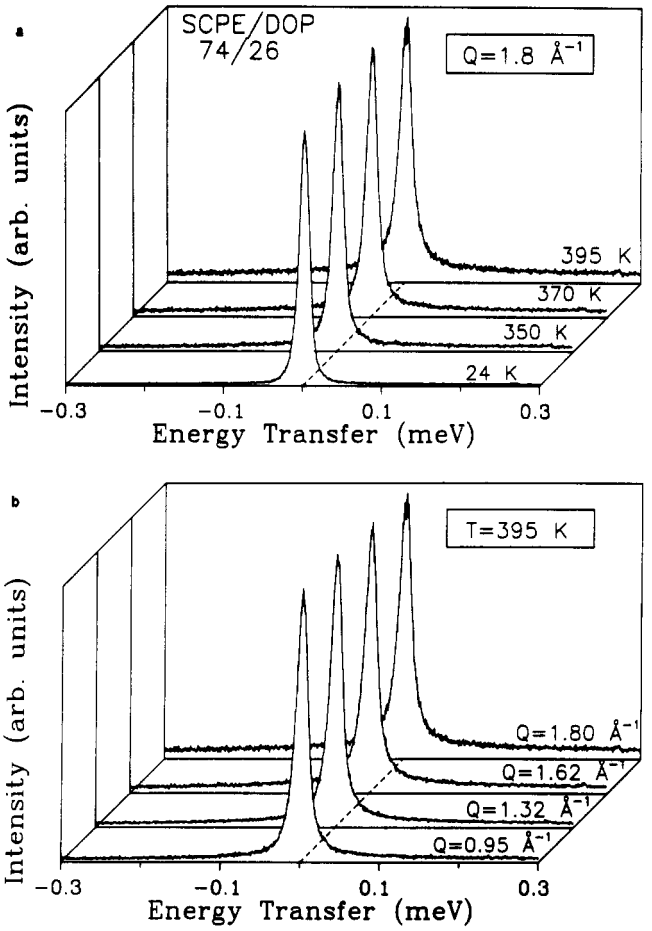

Figure 4. Incoherent neutron scattering spectra of plasticized SCPE with 26% DOP (a) as a function of T and (b) as a function of Q.

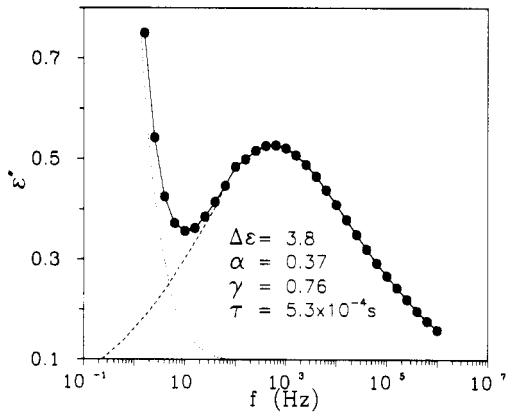

Figure 5. Dielectric loss vs frequency for the primary relaxation of SCPE/DOP (74/26) at $T = 313$ K using the Havriliak–Negami equation (eq 1) and the conductivity contribution. The solid line represents the fit by the superposition of the conductivity (···) and relaxation process (- - -) to the data.

times. In a log ϵ''–log f plot, α and $\alpha\gamma$ give respectively the low- and high-frequency slopes of the relaxation function. According to a recently published model[19] for the shape of the dielectric primary (α) relaxation of polymers, the low- and high-frequency slopes are associated respectively with large- and small-scale modes. In the next section we will compare our results for the shape parameters with this model. The uncertainty in the values of $\Delta\epsilon$ ($=\epsilon_0 - \epsilon_\infty$), α, γ, and τ_{HN} is 2%, 5%, 7%, and 6%, respectively.

The HN function (eq 1) being a four-parameter fit ($\Delta\epsilon$, τ_{HN}, α, and γ) with two parameters to characterize the shape of the distribution provides an excellent fit of the dielectric loss curves (Figures 1 and 5) at all temperatures. However, some theoretical models use a single parameter to characterize the distribution of relaxation times. This is usually the exponent of the Kohlrausch–Williams–Watts (KWW) function

$$g(t) = a \exp(-t/\tau_{KWW})^{\beta_{KWW}} \qquad 0 < \beta_{KWW} \leq 1 \tag{2}$$

which provides a good fit to time-domain relaxation experiments. It has been discussed earlier[20] that, although eqs 1 and 2 can—to certain parameter combinations—deliver similar numerical results, they are not mathematically equivalent. This is because in the HN function two parameters are employed which describe the slope of the low- and high-frequency wing of $\epsilon''(\omega)$, while in the KWW approach the width of the loss curve is considered only. If, on the other hand, the parameter β_{KWW} is needed for the comparison with the theoretical models, then it is possible to extract β_{KWW} through the Fourier transform of the complex permittivity

$$\frac{\epsilon^*(\omega) - \epsilon_\infty}{\epsilon_0 - \epsilon_\infty} = \int_0^\infty \left[-\frac{d\Phi(t)}{dt}\right] e^{-i\omega t}\, dt \tag{3}$$

where $\Phi(t)$ is the normalized relaxation function which describes the randomization of the dipole moment vector in time due to molecular motion. Therefore, neglecting cross-correlations between different chains, the normalized autocorrelation function, $\Phi(t)$, is determined

$$\Phi(t) = \frac{\sum_{ij}^{N} \langle \mu_i(0)\, \mu_j(t) \rangle}{\sum_{ij}^{N} \langle \mu_i(0)\, \mu_j(0) \rangle} \tag{4}$$

where $\mu_j(t)$ denotes the elementary dipole moment in the chain at time t and dipoles i and j are contained in the same chain. From eq 1 the imaginary part $\epsilon''(\omega)$ of the complex dielectric function was calculated from[18]

$$\epsilon''(\omega) = (\epsilon_0 - \epsilon_\infty) r^{-\gamma} \sin \gamma\Psi \tag{5}$$

$$r^2 = 1 + 2(\omega\tau)^\alpha \cos(\alpha\pi/2) + (\omega\tau)^{2\alpha} \tag{6}$$

$$\tan \Psi = \frac{(\omega\tau)^\alpha \sin(\alpha\pi/2)}{1 + (\omega\tau)^\alpha \cos(\alpha\pi/2)} \tag{7}$$

The time-correlation function $\Psi(t)$ was then calculated numerically by a half-sided cosine transformation

$$\Phi(t) = \frac{2}{\pi} \int_0^\infty \frac{\epsilon''(\omega)}{(\epsilon_0 - \epsilon_\infty)} \frac{\cos \omega t}{\omega}\, d\omega \tag{8}$$

after substituting the expression for $\epsilon''(\omega)$ (eq 5) at different temperatures. The resulting function $\Phi(t)$, which is asymmetric in time, is then fitted with the KWW function, and the exponent β_{KWW} is extracted for different temperatures.

In the dynamic mechanical measurements, the loss modulus reaches its maximum value at a frequency ω different than τ^{-1}, because of the broad distribution. Therefore, we have corrected[21] our $\langle\tau\rangle$ measured by mechanical relaxation using the distribution parameter β_{KWW} ($\approx$0.3). The latter was obtained by Fourier transformation of eq 2 in the frequency domain and comparison with G' and G'' in the softening region. This value of β_{KWW} is in good agreement with the distribution obtained from the dielectric experiment.

In the neutron scattering experiment, after making corrections for detector, monitor efficiency, and back-

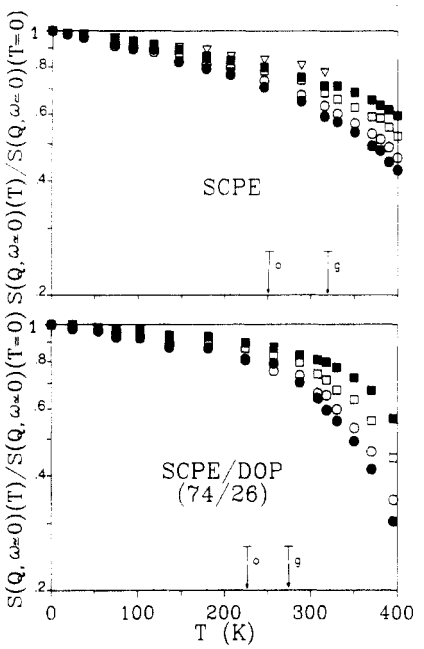

Figure 6. Temperature dependence of the incoherent dynamic structure factor $S(Q,\omega\approx0)$ of (a) SCPE and (b) SCPE/DOP (74/26) normalized to its value at 0 K, plotted for selected Q values. Data points are averaged within an interval of ±0.1 Å around Q = 0.53 (▽), 0.95 (■), 1.32 (□), 1.62 (○), and 1.8 Å^{-1} (●).

ground effects, the measured time-of-flight (TOF) spectrum was converted to a differential scattering cross section $\partial^2\sigma/\partial\Omega\partial E$, where $\partial\Omega$ is the solid angle and ∂E the energy interval for scattered neutrons. The incoherent scattering law $S_{inc}(Q,\omega)$ was then calculated through

$$S_{inc}(Q,\omega) = \frac{k_i}{k_f}\frac{1}{(\langle b^2\rangle - \langle b\rangle^2)}\frac{\partial^2\sigma}{\partial\Omega\partial E} \qquad (9)$$

where k_i and k_f are the incident and scattered wavevectors, respectively, and b is the scattering length for hydrogen atoms. In the present study we have set the spectrometer in a mode where only neutrons with nearly zero energy transfer are counted, giving $S(Q,\omega\approx0)$. This quantity was measured for different Q values as a function of temperature. Values normalized to the extrapolated intensity at 0 K are shown in Figure 6 for the bulk polymer and the SCPE/DOP (74/26) solution. There are two intriguing features in Figure 6. First, there is the strong decrease of the elastic intensity with increasing T and Q (at $T > T_g$). Second, this decrease is more pronounced in the plasticized polymer. The strong decrease of the elastic intensity at high T is consistent with the observed quasielastic broadening and the higher background of the spectra (Figures 3a and 4a). In fact, the lost elastic intensity reappears into the energy window of the spectrometer as an increasing background (with both T and Q) and as a quasielastic broadening which is more pronounced in the plasticized polymer (Figure 4a). These features of the experimental data will be discussed later in more detail.

Results and Discussion

The dynamic mechanical measurements for the bulk and plasticized polymer (Figure 2) exhibit two interesting features: first, the suppression of the β relaxation in comparison with poly(vinyl chloride) (PVC) and, second, the reduced glass transition of the mixture with respect to the bulk polymer. PVC is known to have a low-temperature mechanical relaxation[22] (tan δ maximum at T_{max} = −60 °C and at 1 Hz) which is believed to arise from localized modes of motion. The random distribution of chlorine atoms in SCPE must be related to the suppression of the β relaxation. In other words, the low-T peak in PVC may arise from correlations between side groups from neighbor segments, and these correlations are disrupted by the random chlorine distribution. The suppression of the β relaxation from the mechanical spectra is supported by both the dielectric and neutron scattering measurements. The dielectric β relaxation of PVC has been studied as a function of T[23,24] and pressure (P).[24] The magnitude of the dielectric dispersion was reduced with decreasing T and increasing P. However, the dielectric measurements on SCPE (Figure 1) show no evidence of a secondary relaxation.[25] Similarly, the incoherent neutron scattering measurements for SCPE (Figure 6a) made at higher frequencies exhibit very small mobility in the glassy state as is revealed by the absence of an extra decrease of the elastic intensity beyond the normal decrease expected for a Debye solid. On the other hand, the absence of sub-T_g dielectric relaxations in the present system makes our discussion of the primary (α) relaxation less complicated.

The second feature of the mechanical measurements (Figure 2), i.e., the reduction of the T_g in the solution, is a manifestation of the plasticizer effect on the polymer dynamics. An intriguing feature related to this effect is the broadening of the primary relaxation with plasticization. The broadening of the α peak in the solutions with respect to the bulk polymer has been observed in the dielectric measurements and will be discussed later.

The dielectric measurements on SCPE and SCPE/DOP solutions revealed the existence of a single but broad relaxation peak (Figures 1 and 5). The existence of a single $\epsilon''(\omega)$ peak in all DS data indicates that the polymer/diluent system is miscible—no evidence of microphase separation—at least in the concentrated regime studied here. This is compatible with a single T_g from the DSC measurements and with a single primary peak in the mechanical spectra (Figure 2), and it reveals that the polymer segments and solvent molecules move cooperatively.[26] It is worth mentioning that in the present system the polymer and the diluent both possess dipole moments and microphase separation into SCPE-rich and DOP-rich phases could easily be detected. The HN equation (eq 1) was employed to fit the broad and asymmetric $\epsilon''(\omega)$ spectra, and the four parameters were extracted from the fit: τ_{HN}, $\Delta\epsilon$, α, and γ. We are mainly interested in the temperature and concentration dependence of these parameters. The temperature dependence of the average relaxation time is strongly non-Arrhenius and conforms to the VFT equation

$$\log\tau = \log\tau_0 + \frac{B}{T - T_0} \qquad (10)$$

where $\log\tau_0$, B ($=c_1c_2$), and T_0 ($=T_g - c_2$) are characteristic parameters and c_1 and c_2 are the WLF coefficients. In eq 10, T_0 is the "ideal" glass transition temperature, i.e., an experimentally inaccessible temperature in the limit of infinitely slow cooling. It has been pointed out earlier that, contrary to the DSC-determined T_g, which is not a fundamental quantity in that it shifts with experimental time scales, the value of T_0 is independent of the time scale and therefore is a measure of the properties of the sample.

The temperature dependence of the primary relaxation time is shown in Figure 7 for the bulk polymer, the neat solvent, and two of their mixtures. For the bulk polymer, the strong conductivity contribution to $\epsilon''(\omega)$ excludes measurements at lower frequencies. However, the mechanical relaxation measurements extend the frequency range to lower frequencies, and the two sets of primary relaxation times are in good agreement. It is worth noticing

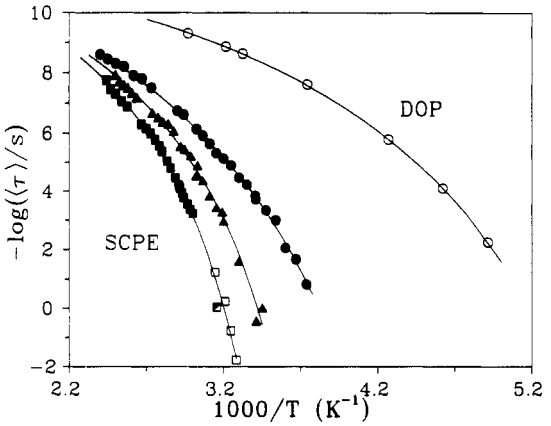

Figure 7. Temperature dependence of the relaxation time τ_{HN} obtained from the fit to eq 1 for bulk SCPE (■), neat DOP (○), and two SCPE/DOP mixtures with concentration 74% (▲) and 59% (●), respectively. The low-frequency data points for SCPE (□), from G''; ⧈, from E'') are from the dynamic mechanical measurements on the same sample. Solid lines are fits to the VFT equation (eq 10). Data points for the 88% sample are omitted for clarity.

Table I
VFT Parameters for the Bulk and Plasticized SCPE

W_{SCPE}	$-\log \tau_0$	B (K)	T_0 (K)
1	12.7 ± 0.2	804 ± 60	249 ± 3
0.88	11.4 ± 0.4	644 ± 85	239 ± 6
0.74	12.5 ± 0.1	770 ± 45	231 ± 2
0.59	12.8 ± 0.2	951 ± 49	188 ± 3
0	12.3 ± 0.1	569 ± 40	147 ± 2

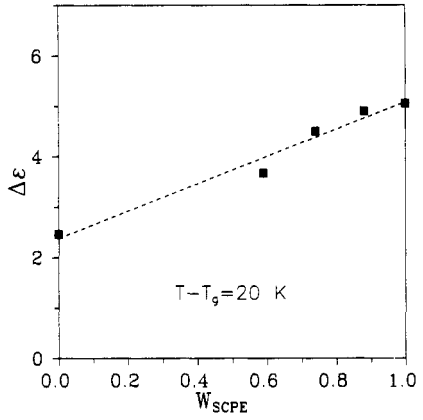

Figure 8. Concentration dependence of the relaxation strength, obtained from the fit to the $\epsilon''(f)$ data (eq 1), at $T - T_g = 20$ K. The dotted line represents a linear interpolation between the two extremes.

that the VFT equation adequately describes $\tau(T)$ over a broad frequency/temperature range. The VFT parameters are given in Table I. The concentration dependence of T_0 is given—within experimental error—by a simple interpolation between the two extremes. This is also reflected in the T_g's, which implies a constant c_2 value: $\langle c_2 \rangle = 57 \pm 9$.

The magnitude of the dielectric dispersion ($\Delta\epsilon$) for the primary relaxation process obtained from the fit to eq 1 is plotted in Figure 8 as a function of polymer concentration, at a temperature equidistant from the individual T_g's. At a given temperature $\Delta\epsilon \sim N\mu^2$, where N is the number of monomers per unit volume and μ is the dipole moment per monomer. Therefore, in view of the results shown in Figure 8, the relaxation strength in the SCPE/DOP mixtures can be obtained by a linear interpolation between the bulk polymer and neat solvent values. This is at variance from the DS measurements on the systems polystyrene/toluene[27] and PVC/tetrahydrofuran,[28] where the magnitude of the dispersion was independent of

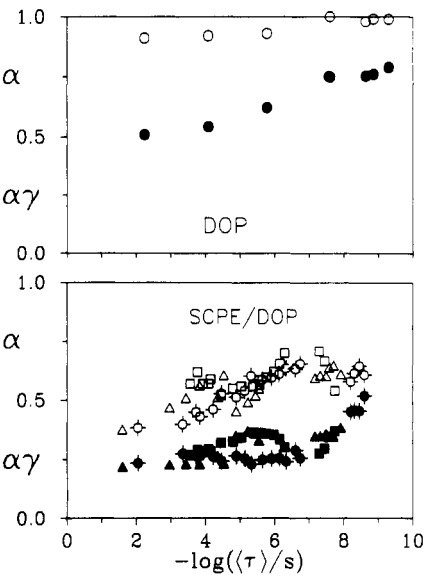

Figure 9. Frequency dependence of the Havriliak–Negami shape parameters for (a) the neat solvent (○, ●), (b) the bulk polymer (□, ■), and the solutions SCPE/DOP (74/26) (△, ▲) and SCPE/DOP (59/41) (-◇-, -◆-).

polymer concentration for polymer concentration higher than 60% but similar to that of the poly(methyl methacrylate)/toluene[29] system.

In Figure 9 we plot the shape parameters of the HN equation (eq 1) as a function of the frequency. An intriguing feature of Figure 9 is the different values of the parameters α and $\alpha\gamma$ for the neat solvent and the polymer solutions. This behavior of the low- and high-frequency slopes of the HN function has been predicted by a recent model[19] for the shape of the primary dielectric relaxation function. The model relates the high-frequency dependence of the dielectric loss curve to the local chain dynamics and the low-frequency dependence to the intermolecular correlations. The main predictions of the model for the shape parameters m ($=\alpha$) and n ($=\alpha\gamma$) are as follows: (i) for low molecular weight substances, in dilute solution, $m = n = 1$ due to the absence of intermolecular long-scale correlations; (ii) for polymers in dilute solution, $m = 1$ and $n = 0.5$ due to intramolecular interactions; (iii) for bulk polymers, $m < 1$ and $n \leq 0.5$. Our results for the glass-forming liquid DOP (Figure 9a) show that $m \approx 1$ and n increases with temperature from 0.5 at $T \approx T_g$ to 0.8 at the highest measurement temperature, in good agreement with recently published data for propylene glycol.[30] For SCPE, m and n display a weak T dependence, with the two parameters being within the predicted range ($m < 1$ and $n \leq 0.5$). For the SCPE/DOP solutions and at low frequencies, m and n assume lower values than in the bulk polymer, but at higher frequencies the situation for n is reversed: $n_{SCPE} < n_{mixture} \leq 0.5$. This last observation implies a stronger T dependence of n and m in the mixtures than in the bulk polymer. It is noteworthy that the monotonic increase of m and n is expected from the model: increasing T decreases the intermolecular interaction (increase of m) and reduces the hindrance of diffusion (increase of n). Furthermore, from the present polymer/diluent system we have evidence of a broader distribution at low temperatures/frequencies than in bulk SCPE and neat DOP.

The broadening of the α relaxation at temperatures near T_g has been observed in polymer blends[31] and polymer/diluent systems[26b,32] and is the subject of a model based on concentration fluctuations.[33] According to this model the sample is divided into subvolumes V_a and the concentration distribution $P(\phi_i)$ of component A in the

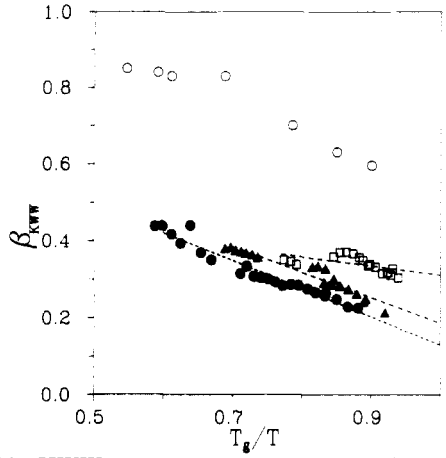

Figure 10. KWW exponent β (eq 2) for bulk SCPE (□), neat DOP (○), and two SCPE/DOP mixtures with SCPE concentration 74% (▲) and 59% (●) versus reduced temperature.

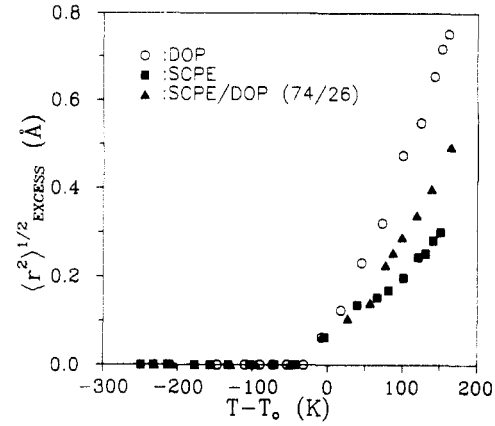

Figure 11. Square-root of the excess mean-square displacement ($\langle r^2 \rangle^{1/2}_{excess}$) calculated from eq 11 after subtracting the normal DWF from low T, for DOP (○), SCPE (■), and SCPE/DOP (74/26) (▲) versus $T-T_0(W)$, where $T_0(W)$ is the ideal glass transition temperature of the neat solvent, the bulk polymer, and the plasticized polymer.

ith subvolume is assumed to be Gaussian. The variance of the distribution ($=\langle \delta\phi^2 \rangle^{1/2}$) is a free parameter in this model and is obtained from the evaluation of the measured dielectric loss curves at different temperatures. The temperature dependences of the concentration fluctuations in the mixtures of poly(vinyl methyl ether) (PVME) with polystyrene (PS)—where only one component is polar (PVME)—were dominated by the temperature dependence of the volume V_a of the cooperatively rearranging units. Application of this model to the present system—where both components are polar—will be the subject of a separate study.

To compare our DS results for the distribution of relaxation times with theoretical models which use a single parameter to characterize the distribution of relaxation times, we have extracted a dipole moment correlation function $\Phi(t)$ from the experimental $\epsilon''(\omega)$ data (eq 3) with the procedure described in the data analysis. The resulting function $\Phi(t)$ was then fitted in the time domain by the KWW decay function (eq 2). This approach has been successfully employed earlier.[12] The stretched exponent β_{KWW}, obtained from the fit to eq 2, is shown in Figure 10 for the bulk polymer, the neat solvent, and two mixtures as a function of T_g/T. Evidently, the T dependence of β_{KWW} is strong, especially for the mixtures. This is in good agreement with the T dependence of the HN shape parameters, and our earlier claim about the equivalence of the two representations for the present system is justified. It is worth mentioning at this point that a systematic T dependence of the distribution of relaxation times has been reported for glass-forming liquids,[34] a molten salt,[35] and polymers.[14] We have used a form linear in T_g/T, i.e., $\beta_{KWW} = A - B(T_g/T)$ (shown in Figure 10) to represent the T dependence of the distribution of relaxation times with (A, B) parameters: (0.55, 0.24) for SCPE, (0.86, 0.67) for SCPE/DOP (74/26), and (0.86, 0.73) for SCPE/DOP (59/41).

Our results for $\beta_{KWW}(T)$ can now be discussed in terms of theoretical models (coupling model,[7] phase-space model,[8] fluctuation approach,[4,6] two-spin facilitated model[9]) which predict a T-dependent β_{KWW}. More specifically, a phase-space percolation model predicts a stretched exponential decay (eq 2) below an upper temperature where $\beta_{KWW} = 1$ (Debye relaxation) to an exponent tending to $1/3$ as we approach T_g. However, our data give evidence for lower β_{KWW} values at $T \approx T_g$ with values of 0.31, 0.19, and 0.13 respectively for SCPE, SCPE/DOP (74/26), and SCPE/DOP (59/41). Such very broad distributions of relaxation times at $T \approx T_g$ are expected from the model based on concentration fluctuations[33] discussed earlier. Similarly, in the coupling model, the fluctuation approach, and the two-spin facilitated model, the lowest β_{KWW} value can be less than $1/3$. For example, in the latter model[9b] a value of 0.2 is plausible, whereas in the fluctuation approach not only the mean relaxation time (eq 10) but also the exponent β_{KWW} is governed by the VFT equation, i.e., $\beta_{KWW} \sim T - T_0$, and the distribution of relaxation times diverges at T_0. This prediction is valid for the SCPE/DOP mixtures but not for the bulk polymer which possesses a nonvanishing β_{KWW} ($\sim$0.24) at $T = T_0$. This has been discussed in the latter model[6] as being due to the hindered increase of the length scale $\xi(T)$ because of entanglements which leads to a significant widening of the spectrum, at low T. We mention here that our values of β_{KWW} at T_g and T_0 are obtained by extrapolation from higher T—assuming a linear behavior—and therefore are subject to some uncertainty.

Alternatively, the temperature T_0 which is not easily accessible in dynamic experiments can be reached using incoherent neutron scattering. In the neutron scattering experiment we monitored the elastic scattering intensity $S(Q,\omega\approx0)$ at different Q values as a function of T. In this way the normalized elastic intensity was obtained and plotted in Figure 6, for the bulk polymer and the SCPE/DOP (74/26) solution. At low T, far below T_g, the elastic intensity can be described by the Debye model for harmonic solids, i.e.

$$S(Q,\omega) \sim e^{-\langle r^2 \rangle Q^2}, \quad \langle r^2 \rangle \sim T \tag{11}$$

where $\langle r^2 \rangle$ is the mean-square displacement due to vibrations. Therefore, $\ln [S(Q,\omega\approx0)(T)/S(Q,\omega\approx0)(T\approx0)] \sim -T$ according to the Debye–Waller factor (DWF), and our experimental data for SCPE (Figure 6a) and SCPE/DOP (74/26) (Figure 6b) agree with this prediction at sufficiently low temperatures. The extra decrease of the elastic intensity beyond that expected from eq 11 sets in at temperatures below T_g and becomes strongly Q-dependent at higher T. This "extra" decrease of the elastic intensity has been observed in a number of systems before: both glass-forming liquids[36-38] and polymers[39,40] show this feature. However, to our knowledge, this decrease has not been reported before to correlate with T_0.

To quantify this effect, we plot in Figure 11 the square-root of the excess mean-square displacement as a function of temperature difference from T_0, where T_0 is the ideal glass transition temperature given in Table I. $\langle r^2 \rangle^{1/2}_{excess}$ is calculated from eq 11, after subtracting the low-T DWF due to vibrations. The remaining quantity represents

proton mobility due to motion and contains the complete Q information. The decrease of the elastic intensity (Figure 6) and the concomitant increase of $\langle r^2 \rangle^{1/2}$ (Figure 11) sets in at a temperature $T \approx T_0$ for a low molecular weight liquid (DOP), a polymer (SCPE), and their mixture SCPE/DOP (74/26). We should mention at this point that the observed correlation between proton mobility and T_0, as obtained by independent neutron scattering and dielectric measurements on the same samples, is surprising. The neutron scattering experiment is made at high frequencies (Figures 3 and 4, 1 meV $\approx 2.4 \times 10^{11}$ Hz), and in this frequency range low-T relaxations are likely to contribute. However, in the present system such relaxations are suppressed as inferred by the mechanical and dielectric measurements. Additionally, low-T relaxations can exist below T_0, whereas in the present system the mobility at $T \leq T_0$ is solely due to the DWF. An alternative interpretation can be given in terms of the "fast" β process of the mode coupling theory (MCT).[10] MCT predicts a dynamic instability at a temperature T_c, above the calorimetric T_g. Above T_c two distinct relaxation processes (α and β) exist in the density correlation function, whereas below T_c only the fast β process exists, which give rise to an anomalous DWF. However, in the present system the HN and KWW parameters tend to increase with increasing T (Figures 9 and 10). This implies that a master curve construction using the time–temperature superposition is incorrect, at least for the mixtures. It has been suggested[41] that our data for the distribution of relaxation times could refer to $T < T_c$ since for complex polymeric systems there is no ad hoc knowledge of where T_c is—if it exists at all.

Conclusions

The dynamics of concentrated solutions of solution-chlorinated polyethylene with bis(2-ethylhexyl) phthalate have been studied over a broad temperature/frequency range with dielectric spectroscopy and incoherent neutron scattering. The main results of the present study are as follows:

(i) There exists only one primary (α) relaxation in these homogeneous concentrated solutions due to cooperative motion of polymer segments with solvent molecules.

(ii) The T dependence of the dynamics in the SCPE/DOP mixtures is adequately described by the VFT equation over a broad temperature range.

(iii) A broader distribution of relaxation times has been observed in the mixtures with respect to the bulk polymer and neat solvent at $T \approx T_g$.

(iv) The distribution of relaxation times in the SCPE/DOP solutions obtained either in the frequency domain (HN parameters α and γ) or in the time domain (KWW parameter β) displays a systematic T dependence and diverges at T_0. For the bulk polymer the T dependence is weaker with a nonzero value at T_0. Our results for the T dependence of the distribution of relaxation times are in good agreement with theoretical models which predict a narrowing of the distribution at high T.

(v) From the incoherent neutron scattering measurements, made on the same samples at a higher frequency range, we find that the proton mobility correlates surprisingly well with the characteristic temperature T_0 of the VFT approach.

Acknowledgment. G.F. thanks Professors E. Donth and W. Götze for helpful suggestions and the Max-Planck-Institut für Polymerforschung for its hospitality. We thank Dr. T. Pakula for the mechanical measurements on the bulk polymer. Financial support by the Science and Engineering Research Council and the German Science Foundation (Sonderforschungsbereigh 262) is highly appreciated.

References and Notes

(1) Adam, G.; Gibbs, J. H. *J. Chem. Phys.* **1965**, *43*, 139.
(2) Adachi, K. *Macromolecules* **1990**, *23*, 1816.
(3) Matsuoka, S.; Quan, X. *Macromolecules* **1991**, *24*, 2770.
(4) Donth, E. *J. Non-Cryst. Solids* **1982**, *53*, 325.
(5) See for example: Williams, G. *J. Non-Cryst. Solids* **1991**, *131–133*, 1.
(6) Schick, C.; Donth, E. *Phys. Scr.* **1991**, *43*, 423.
(7) Ngai, K. L.; Rendell, R. W.; Rajagopal, A. K.; Teitler, S. *Ann. N.Y. Acad. Sci.* **1986**, *484*, 150.
(8) Campbell, I. A.; Flesselles, J.-M.; Jullien, R.; Botet, R. *Phys. Rev. B.* **1988**, *37*, 3825.
(9) (a) Fredrickson, G. H.; Andersen, H. C. *Phys. Rev. Lett.* **1984**, *53*, 1244. (b) Fredrickson, G. H.; Brawer, S. A. *J. Chem. Phys.* **1986**, *84*, 3351.
(10) (a) Leutheusser, E. *Phys. Rev. A* **1984**, *29*, 2765. (b) Bengtzelius, U.; Götze, W.; Sjölander, A. *J. Phys. C* **1984**, *17*, 5915. (c) Götze, W. In *Liquds, Freezing and the Glass Transition*; Hansen, J. P., Levesque, D., Zinn-Justin, J., Eds.; North-Holland: Amsterdam, The Netherlands, 1991.
(11) Floudas, G.; Fytas, G.; Fischer, E. W. *Macromolecules* **1991**, *24*, 1955.
(12) Boese, D.; Momper, B.; Meier, G.; Kremer, F.; Hagenah, J.-U.; Fischer, E. W. *Macromolecules* **1989**, *22*, 4416.
(13) Meier, G.; Gerharz, B.; Boese, D.; Fischer, E. W. *J. Chem. Phys.* **1991**, *94*, 3050.
(14) Floudas, G.; Fytas, G.; Alig, I. *Polymer* **1991**, *32*, 2307.
(15) Duggal, A. R.; Nelson, K. A. *J. Chem. Phys.* **1991**, *94*, 7677.
(16) Chai, Z. Ph.D. Thesis, Imperial College, London, 1982.
(17) Kremer, F.; Boese, D.; Meier, G.; Fischer, E. W. *Prog. Colloid Polym. Sci.* **1989**, *80*, 129.
(18) Havriliak, S.; Negami, S. *Polymer* **1967**, *8*, 101.
(19) Schönhals, A.; Schlosser, E. *Colloid Polym. Sci.* **1989**, *267*, 125.
(20) Macdonald, J. R.; Hurt, R. L. *J. Chem. Phys.* **1986**, *84*, 496.
(21) Patterson, G. D.; Lindsey, C. P. *Macromolecules* **1981**, *14*, 83.
(22) Heijboer, J. *Int. J. Polym. Mater.* **1977**, *6*, 11.
(23) Ishida, Y. *Kolloid Z.* **1960**, *168*, 29.
(24) Williams, G.; Watts, D. C. *Trans. Faraday Soc.* **1971**, *67*, 1971.
(25) Dielectric measurements on lightly (up to ca. 4/100 Cl/CH_2) chlorinated polyethylenes (crystalline) have been reported: (a) Matsuoka, S.; Roe, R. J.; Cole, H. F. In *Dielectric Properties of Polymers*; Karasz, F. E.; Ed.; Plenum Press: New York, 1972. (b) Ashcraft, C. R.; Boyd, R. H. *J. Polym. Sci., Polym. Phys. Ed.* **1976**, *14*, 2153.
(26) Two-primary (α) relaxations have been recently reported in two polymer/diluent systems: (a) poly(methyl methacrylate)/toluene [Floudas, G.; Fytas, G.; Brown, W. *J. Chem. Phys.* **1992**, *96*, 2164]; (b) polystyrene/bis(2-ethylhexyl)phthalate [Floudas, G.; Steffen, W.; Giebel, L.; Fytas, G. *Colloid Polym. Sci.*, in press].
(27) Adachi, K.; Fujihara, I.; Ishida, Y. *J. Polym. Sci., Polym. Phys. Ed.* **1975**, *13*, 2155.
(28) Adachi, K.; Ishida, Y. *J. Polym. Sci., Polym. Phys. Ed.* **1976**, *14*, 2219.
(29) Adachi, K.; Kotaka, T. *Polym. J.* **1981**, *13*, 687.
(30) Schönhals, A.; Kremer, F.; Schlosser, E. *Phys. Rev. Lett.* **1991**, *67*, 999.
(31) Zetsche, A.; Kremer, F.; Jung, W.; Schulze, H. *Polymer* **1990**, *31*, 1883.
(32) Fytas, G.; Floudas, G.; Ngai, K. L. *Macromolecules* **1990**, *23*, 1104.
(33) Fischer, E. W.; Zetsche, A. *Polym. Prepr. (Am. Chem. Soc., Div. Polym. Chem.)* 1992.
(34) Dixon, P. K.; Nagel, S. R. *Phys. Rev. Lett.* **1988**, *61*, 341.
(35) Cheng, L.-T.; Yan, Y.-X.; Nelson, K. A. *J. Chem. Phys.* **1989**, *91*, 6052.
(36) Bartsch, E.; Fujara, F.; Kiebel, M.; Sillescu, H.; Petry, W. *Ber. Bunsenges. Phys. Chem.* **1989**, *93*, 1252.
(37) Floudas, G.; Higgins, J. S.; Fytas, G. *J. Chem. Phys.* **1992**, *96*, 7672.
(38) Fujara, F.; Petry, W. *Europhys. Lett.* **1987**, *4*, 921.
(39) Frick, B.; Richter, D.; Petry, W.; Buchenau, U. *Z. Phys. B* **1988**, *70*, 73.
(40) Meier, G.; Fujara, F.; Petry, W. *Macromolecules* **1989**, *22*, 4421.
(41) Götze, W., private communication.